Published in final edited form as:
Mol Pharm. 2010 June 7; 7(3): 884–893. doi:10.1021/mp100029t.

Trigeminal pathways deliver a low molecular weight drug from the nose to the brain and orofacial structures

Neil J. Johnson, **Leah R. Hanson**, and **William H. Frey II***

Abstract

Intranasal delivery has been shown to non-invasively deliver drugs from the nose to the brain in minutes along the olfactory and trigeminal nerve pathways, bypassing the blood-brain barrier. However, no one has investigated whether nasally applied drugs target orofacial structures, despite high concentrations observed in the trigeminal nerve innervating these tissues. Following intranasal administration of lidocaine to rats, trigeminally-innervated structures (teeth, temporomandibular joint (TMJ), and masseter muscle) were found to have up to 20-fold higher tissue concentrations of lidocaine than the brain and blood as measured by ELISA. This concentration difference could allow intranasally administered therapeutics to treat disorders of orofacial structures (i.e. teeth, TMJ, and masseter muscle) without causing unwanted side effects in the brain and the rest of the body. In this study, an intranasally administered infrared dye reached the brain within 10 minutes. Distribution of dye is consistent with dye entering the trigeminal nerve after intranasal administration through three regions with high drug concentrations in the nasal cavity: the middle concha, the maxillary sinus, and the choana. In humans the trigeminal nerve passes through the maxillary sinus to innervate the maxillary teeth. Delivering lidocaine intranasally may provide an effective anesthetic technique for a non-invasive maxillary nerve block. Intranasal delivery could be used to target vaccinations and treat disorders with fewer side effects such as tooth pain, TMJ disorder, trigeminal neuralgia, headache, and brain diseases.

Keywords

intranasal; brain; maxillary sinus; orofacial; masseter muscle; lidocaine; infrared dye; migraine; temporomandibular disorder; tooth pain; trigeminal neuralgia

Introduction

Intranasal delivery provides a non-invasive method of bypassing the blood-brain barrier to rapidly deliver therapeutic agents to the brain, spinal cord, lymphatics and to the vessel walls of the cerebrovasculature for treating CNS disorders such as Alzheimer's disease, brain tumors, and stroke.[1–6] This novel delivery method allows drugs, therapeutic proteins, polynucleotides, and viral vectors that do not normally cross the blood-brain barrier to be delivered to the central nervous system.[7, 8] Additionally, intranasal targeting of drugs to the CNS avoids first pass elimination by the liver allowing a lower therapeutic drug dose and fewer systemic side effects. Delivery from the nose to the central nervous system occurs within minutes along both the olfactory and trigeminal nerves.[7, 9, 10] Delivery occurs by an extracellular route and does not require that the drugs bind to any receptor or undergo axonal transport. Intranasal delivery has been reported to effectively bypass the blood-brain barrier and treat neurologic disorders in mice, rats, primates, and humans.[2, 9–12] In humans, intranasal delivery has been documented

*Alzheimer's Research Center at Regions Hospital, HealthPartners Research Foundation, 640 Jackson Street, Mailstop: 11203A, Saint Paul, MN 55101, 612-261-1998 Tel, 651-254-3661 Fax, alzheimr@umn.edu.

to transport neuropeptides to the CSF.[13] Furthermore, intranasal insulin has been shown to improve memory in healthy adults, obese men, and Alzheimer's patients.[11, 14–20] Although considerable intranasal studies have focused on nose to brain delivery, no studies have investigated if drug delivery occurs to orofacial structures innervated by the trigeminal nerve despite evidence that high drug concentrations are observed in the trigeminal nerve.

Evidence suggests that after intranasal administration, the olfactory and trigeminal nerves receive high concentrations of drug from the nasal cavity and transport it to the brain and other connected structures.[7] Intranasally administered drug can reach the trigeminal nerves and perineural space from the absorbent respiratory and olfactory pseudoepithelium because they are innervated by the trigeminal nerve. Chemuturi & Donovan 2007 demonstrated that intranasal delivery rapidly fluxes dopamine (a small molecule) across the nasal pseudoepithelium where large trigeminal nerve branches pass.[21] Additionally, the trigeminal nerve covers and travels through the maxillary sinus, which is connected to the nasal cavity and is also lined by a thin pseudoepithelium. It is not known where drug enters the trigeminal nerve from the nasal cavity, but Thorne et al 2004 reported an increase in IGF-I concentrations in the three major branches of the trigeminal nerve and in the brain stem where the trigeminal nerve enters following intranasal IGF-I administration. This suggests that intranasal delivery uses the trigeminal nerve pathway as a conduit to transport drug to the brainstem beginning at the entry through the pons and then through the rest of the hindbrain.[22] A portion of the trigeminal nerve that passes through the cribriform plate may also contribute to delivery of drug from the nasal mucosa to the forebrain.[7] If the trigeminal nerve can transport drug to the forebrain and hindbrain, connected structures, then trigeminally innervated structures such as the teeth, masseter muscle, and TMJ may also receive drug from the trigeminal nerve. Even though drug is transported to the hindbrain, treatment of the trigeminal nerve without affecting the brain may be possible because a 20-fold higher drug concentration has been reported in the trigeminal nerve as compared to the brain.[7, 9] Understanding where drug enters the trigeminal nerve from the nasal cavity after intranasal administration would help target the trigeminal nerve for clinical use.

Intranasal drugs have been used to treat orofacial structures clinically, yet these studies did not describe the trigeminal nerve as a mechanism of drug transport.[23–39] Although local injections can effectively target orofacial structures, there are adverse effects including pain, dental anxiety, and the patient cannot self-administer medication. Although topical and gas anesthesia are helpful in decreasing pain before injection, intranasal delivery may provide a better approach by being rapid, painless, targeted, and patient administered. Intranasal migraine medications (sumatriptan, zolmitriptan) require 1/5 the dose of oral formulations with a more rapid onset and few side effects.[23–35] Furthermore, lidocaine, a drug not usually indicated for migraine or trigeminal neuralgia treatment, was found to be therapeutic when delivered intranasally.[36–39] Finding specific regions in the nasal cavity where drug enters the trigeminal nerve could help develop better devices in clinic to target the trigeminal nerve and connected structures.

In this study, intranasal administration of lidocaine resulted in rapid delivery to the brain, trigeminal nerve and orofacial structures while minimal drug was delivered to the blood as compared to intravenous delivery. The biodistribution of the dye showed high concentrations at three locations near the trigeminal nerve (the middle nasal concha, the maxillary sinus, and choana). Targeting these nasal sites could improve delivery to the brain, trigeminal nerve, or orofacial structures.

Experimental Section

Experiment 1: Concentrations of lidocaine in rat tissues following intranasal and intravenous administration

Experimental Design—Rats were administered the same lidocaine dose intranasally or intravenously. After approximately 30 minutes, rats were perfused, and a variety of brain, orofacial and body structures were dissected to determine lidocaine concentrations. Tissues were pulverized and supernatant fractions were analyzed using an ELISA, as described in detail below.

Animals—Adult male Sprague-Dawley rats (ordered 200–250g from Charles River Laboratories, Wilmington, MA, USA) were group housed under a 12-h light/dark cycle. Food and water was provided ad libitum. Animals were cared for and experiments were approved in accordance with institutional guidelines (Regions Hospital, HealthPartners Research Foundation Animal Care and Use Committee approved protocol 05–052) and the National Institutes of Health Guide for the Care and Use of Laboratory Animals (1996). Lidocaine (8 mg) was either intranasally (n=6) or intravenously (n=6) administered to two groups, while another group (n=3) was given intranasal vehicle (phosphate buffered saline, PBS) to collect tissue for the ELISA standard curve and tissue to be spiked with known concentrations of lidocaine to detect the specificity and sensitivity of the assay.

Intranasal and intravenous delivery—Lidocaine HCl was purchased from Sigma Aldrich (cat# L5647-15G). Animals were anesthetized with pentobarbital sodium (Nembutal, 40 mg/kg I.P.; Abbott Laboratories, North Chicago, IL USA). Core body temperature was maintained at 37 °C using a rectal temperature probe and heating pad. A 20-gauge cannula was inserted into the descending aorta for blood access. For intranasal delivery, rats were laid on their back with a rolled 2″×2″ gauze under the neck to maintain a horizontal head position. During intranasal delivery, a cotton swab wrapped in paraffin was used to occlude one nostril while an 8 μL drop of 10% lidocaine dissolved in phosphate buffered saline (PBS) was placed onto the opposite nostril and naturally sniffed in by the rat. Five drops were administered in each nostril, alternating every two minutes over 18 minutes. A total of 8 mg of lidocaine was given in 80 μL. For intravenous delivery, 80 μL of 10% lidocaine was combined with 0.5 mL of saline, and 1/10 doses were injected through the descending aorta cannula every two minutes for 18 minutes. Every 5 minutes, a 0.25 mL sample of blood was removed from the descending aorta. At 10 & 20 minutes 0.5 mL of saline was administered through the descending aorta cannula to replace lost blood volume.

Tissue collection—After 25 minutes from delivery onset, 120 mL of cold saline was perfused through the descending aorta cannula of the anesthetized rat at 15 mL/min using a syringe pump. After perfusion and death, the head was removed using a guillotine, and tissues were dissected on ice. Blood samples were centrifuged at 16,000 G for 30 minutes and supernatant removed. The deep cervical lymph nodes were removed as described in Thorne et al. 2004. The skin dorsal to the brain cavity was incised at the midline. The whole brain was removed starting caudally and progressing rostrally using a hemostat to remove the skull. The whole brain was dissected in the following order in a petri dish: cerebellum, brainstem, midbrain, diencephalon, and cortex. The olfactory bulb was removed last to minimize contamination. After removing the whole brain, the trigeminal ganglion was removed from the base of the skull without opening the nasal cavity. The lacrimal gland, eye, and masseter muscle were dissected by first removing the overlying skin. The temporomandibular disc was dissected from the mandibular condyle and glenoid fossa. All teeth were extracted with nerves inside pulp. The tongue and tissue from the maxillary sinus were dissected. The nasal epithelium was removed from the cribriform plate after splitting the skull along the midline. The spinal cord

was removed whole and dissected into cervical, thoracic, and lumbar segments without removing the dura. Each liver lobe and the kidney cortex and medulla were dissected. Urine was collected from the bladder using a 1 mL needle syringe. All tissues were placed in tubes, weighed, flash frozen in liquid nitrogen, and stored at −70 °C until tissue preparation for ELISA.

Tissue preparation for ELISA—Tissue was diluted 1:5 (tissue weight (g): homogenization buffer (ml)). Homogenization buffer consisted of Tris HCl (100 mM), sodium chloride (400 mM), 2% bovine serum albumin, and 0.05% sodium azide. Two dozen 1.0 mm glass and zirconium microbeads were added to each tube of tissue and shaken vigorously for three 5-minute increments at ~10 Hz using a motorized microbead shaker. After pulverizing, samples were sonicated until the solution was homogenous. After sonication, the samples were centrifuged at 16,000 G for 30 minutes. Supernatant was removed and flash frozen in liquid nitrogen and stored at −70 °C.

Lidocaine ELISA—Supernatant was allowed to thaw to room temperature and diluted 1:500 in EIA buffer supplied in the lidocaine ELISA kit (Neogen Corporation, Lexington KY). An 8 μL sample was used in the lidocaine ELISA kit well, otherwise the kit instructions were followed. Briefly, enzyme conjugate was diluted 1:180 in EIA buffer, and 180 μL was incubated with the 8 μL sample in each ELISA well (duplicates of each tissue) for 45 minutes. Using a multi-channel pipettor, the wells were washed with buffer, and 150 μL of substrate was incubated for 1.5 hours (all supplied in the kit). At 1.5 hours samples were read using a plate reader (Molecular Devices) at 450 nm after adding 50μL of 1.0 N HCl, which doubles the color intensity read by the plate reader. Samples were compared against a standard curve of lidocaine spiked brain supernatant from vehicle treated animals processed the same way as experimental samples.

Supernatant from vehicle treated animals were spiked with known concentrations of lidocaine to validate the specificity and sensitivity of the assay. A variety of tissues showed the same concentration measured by the assay as the amount injected into the tissues. The assay was very specific to lidocaine as tissues without lidocaine were below the standard curve's sensitivity and had the same optical density as wells filled with distilled water. The lowest detectable concentration was ~10 nM. The standard curve consistently had an R squared value of ≥ 0.99.

Statistical analysis—Data was analyzed and graphed using Prism statistical software (version 5.0; GraphPad, La Jolla, CA). The lidocaine concentrations were quantified using standard curves. An unpaired t-test assuming equal variance was used to compare each tissue between the intranasal and IV groups. P values were determined and represented as <0.05 (*), <0.01 (**), and <0.001(***). Targeting of lidocaine for intranasal or intravenous delivery was calculated by dividing the tissue concentration by the blood's lidocaine concentration at 25 minutes within the same delivery method. A drug-targeting index (DTI) was used to measure improved CNS targeting through intranasal delivery as compared to intravenous delivery and was calculated by determining the ratio of intranasal to intravenous targeting of lidocaine.

Experiment 2: In vivo imaging of intranasally administered IRdye 800 and biodistribution at 30 minutes

Experimental Design—IRdye 800 was intranasally administered to rats and imaged with an infrared imaging system for 30 minutes prior to euthanasia and tissue collection. IRdye 800 was used because it can be imaged in vivo and is easily visible by the naked eye, enabling tracking of the dye (as opposed to lidocaine which is clear in solution). In addition, IRdye 800 fluoresces at 800 nm, a unique wavelength where tissue is relatively transparent because of

minimal absorption by blood and water. IRdye 800 had the closest molecular weight to lidocaine of any of the available infrared dyes.

Animals—Adult male Sprague-Dawley rats (n=3, 200–250g; Charles River Laboratories, Wilmington, MA, USA) were housed under a 12-h light/dark cycle and were cared for as described in Experiment 1.

IRdye 800 and Odyssey infrared imaging system—IRdye 800 (Li-Cor Bioscience, Lincoln, NE) was used for in vivo imaging after intranasal administration. IRdye 800 conjugation sites were neutralized by dilution in PBS (pH 8.5) for greater than two hours. IRdye 800 was imaged using a Li-Cor Odyssey infrared imaging system (Lincoln, NE) equipped for in vivo imaging. Rats were shaved completely with an electric razor to limit the hair absorbing infrared light, which can interfere with imaging. The infrared background was scanned prior to delivery.

Intranasal administration and in vivo imaging—Rats were anesthetized as described in Experiment 1. Drops (8 μL) of 1 mM IRdye 800 in saline were given every 2 minutes for 18 minutes alternating nostrils using the same intranasal technique as experiment 1 for a total of 80 μL administered. The head and neck were scanned between each 2-minute delivery interval. During in vivo imaging, the Odyssey scanner resolution was 337 μm^2/pixel with a scanning depth of 3 ± 0.5 mm for both the 700 nm and 800 nm filters. After 25 minutes the rat was removed from the imaging device and transcardially perfused with 60 mL cold saline followed by 360 mL 4% paraformaldehyde at a rate of 15 mL/min using a syringe pump.

Dissection and subsequent imaging—Following perfusion, the brain was removed, sectioned in 1 mm coronal brain slices using a brain matrix from the olfactory bulb to the upper cervical spinal cord, and imaged. The spinal cord was dissected and imaged whole. The head with brain removed was cut mid-sagittally so the cross-section could be imaged. The trigeminal nerve and respiratory epithelium were removed, and the head was then re-scanned. The trigeminal maxillary nerve branch was dissected from the whisker pad to the brainstem nerve root. The following tissues were also removed and imaged: kidneys, heart, lungs, digestive tract, spleen, liver, urine (1 mL), epididymis, and testes. For all tissues, the scanning resolution after dissection was 21 μm^2/pixel for both 700 nm and 800 nm filters. The scanning depth for thin tissues such as coronal brain slices, spinal cord, skin and aponeurosis was 1 ± 0.5 mm. The rest of the tissues were imaged at 4 ± 0.5 mm scanning depth. Alongside experimental tissues, a standard curve was imaged by scanning known concentrations of IRdye 800 in glass tubes. The known concentrations detected by the Odyssey scanner ranged from 10 nM to 100 μM, otherwise IRdye seen by the naked eye was defined as >100 μM.

Results

Experiment 1: Tissue concentrations of lidocaine following intranasal and intravenous administration

Blood bioavailability of lidocaine was lower following intranasal delivery as compared to intravenous delivery—Although the nose is well vascularized, blood levels of lidocaine were significantly lower following intranasal administration as compared to intravenous administration across the entire 25-minute period (Figure 1). The area under the curve of the lidocaine concentration in the blood was also significantly lower (p=0.0002) following intranasal application (173 μM*minutes) than following intravenous injection (3,916 μM*minutes). Blood concentration of lidocaine peaked at 5 minutes after intravenous administration vs. 10 minutes after intranasal administration; then both steadily decreased. At 25 minutes, the final sample point, lidocaine blood concentrations were significantly lower

(p=0.0168) following intranasal (7.9 μM) vs. intravenous administration (21 μM). The kidney was the only systemic organ where intranasal and intravenous administration was not significantly different (p=0.6525). Intravenous administration resulted in significantly higher lidocaine concentrations in the urine (p=0.0012) and liver (p=0.0015). Intranasal administration resulted in significantly higher concentrations at the drug administration sites such as the nasal epithelium (p=<0.0001). All of the lidocaine concentration data for each group can be found in Table 1.

Brain structures had higher lidocaine concentrations following intranasal delivery as compared to intravenous delivery—In spite of the much higher blood lidocaine levels observed with intravenous administration, intranasal delivery of lidocaine to the brain was significantly higher for all structures except the lumbar spinal cord (Figure 2). Following intranasal administration, the olfactory bulb, connected to the olfactory epithelium via olfactory sensory neurons, received the highest concentration of lidocaine (266 μM), and concentrations decreased in a rostral-to-caudal direction from the cortex (33 μM) to the diencephalon (16 μM) then increased from the midbrain (23 μM) to the brainstem (45 μM), where the trigeminal nerve root and ganglion enters running along the base of the skull (147 μM). The lidocaine concentration decreased in a dorsal direction from the brainstem to the cerebellum (35 μM). Progressing caudally the concentration decreased from the brainstem to the lower cervical spinal cord (24 μM) to the thoracic spinal cord (21 μM) to the lumbar spinal cord (19 μM). In contrast, intravenous administration resulted in lower and fairly similar concentrations throughout the central nervous system structures (7–10 μM), except in the diencephalon (2.0 μM; p= 0.0004).

Orofacial structures had higher lidocaine tissue concentrations than brain structures following intranasal delivery—Intranasal administration delivered significantly more lidocaine to all orofacial structures compared to brain structures, except the facial structures innervated by the ophthalmic branch of the trigeminal nerve (lacrimal gland, eye, and skin on the head). Following intranasal administration, the maxillary sinus (3,508 μM) received the highest lidocaine concentration besides the nasal epithelium (4,549 μM) where the drug is directly deposited. The trigeminal nerve, which passes through the maxillary sinus and the nasal epithelium, had a concentration of 147 μM before it enters the brainstem (at the base of the skull). The trigeminal nerve segment was cut at the base of the skull because dissecting through the nasal epithelium in an unfixed animal would have contaminated the trigeminal nerve. In the IRdye 800 study discussed later, the trigeminal nerve was dissected more rostrally to the teeth and nasal cavity where the concentration was dramatically higher (~100 μM) compared to near the brainstem (~10 μM). The trigeminal nerve concentration near the maxillary teeth is ~1470 μM. This higher concentration in maxillary teeth nerves compared to the rostral part of the trigeminal nerve is due to the close proximity to the maxillary sinus (3,508 μM) and nasal epithelium (4,549 μM). Of the maxillary teeth, incisors (803 μM) received the highest concentration of lidocaine followed by the maxillary molars (476 μM). The maxillary incisors are in closer proximity than the maxillary molars to the middle concha, where the drug is directly deposited. The mandibular teeth are innervated by the trigeminal nerve (147 μM) and close to the mandibular molar branch that innervates the tongue (651 μM). Of the mandibular teeth, the molars (199 μM) received the highest lidocaine concentration of the mandibular trigeminal nerve branch followed by the mandibular incisors (148 μM), which is located further from the tongue (651 μM) and the maxillary nerve branch (147 μM). The mandibular teeth lidocaine concentrations were not significantly different from that of the trigeminal ganglion, while the maxillary teeth had significantly higher concentrations (p<0.05) than the trigeminal ganglion suggesting maxillary teeth are receiving lidocaine from some other source. The intranasal IRdye experiment suggests the maxillary sinus is the main source of drug to the maxillary teeth. The teeth had the highest drug targeting indices (145 to 701) of all

the tissues collected. Intranasal administration delivered less lidocaine to facial structures as compared to oral structures. The temporomandibular joint (72 μM) has a higher density of trigeminal nerve fibers than the masseter muscle (15 μM). The lacrimal gland was not significantly higher in lidocaine concentration following intranasal delivery (58 μM) as compared to intravenous administration (43 μM).

Oral structures had the highest drug-targeting index, followed by brain structures and facial structures—The drug-targeting index (DTI) was highest among the maxillary sinus (856), teeth (maxillary incisors 701; maxillary molars 413; mandibular incisors 145; mandibular molars 270) and tongue (213). Facial structures had a lower DTI; these include temporomandibular joint (27), masseter muscle (8.2), lacrimal gland (3.6), eye (3.4), and skin on the head (2.7). All the central nervous system structures had a drug targeting index (DTI) greater than 1. The highest DTI central nervous system structures were the olfactory bulb (84), diencephalon (22), and brainstem (14). The diencephalon had a significantly lower concentration ($p=0.0004$) compared to other brain structures during intravenous delivery. The DTI of the remaining central nervous system structures are cerebellum (11), lower cervical spinal cord (9.0), cortex (8.9), midbrain (8.4), thoracic spinal cord (6.8), and lumbar spinal cord (3.8).

Experiment 2: In vivo imaging of intranasally administered IRdye 800 and biodistribution at 30 minutes

IRdye 800 was visualized in the brain at 10 minutes following intranasal administration—Prior to intranasal treatment with IRdye 800, rat tissue is almost transparent at 800 nm (Figure 3a). The neck and body were less transparent compared to the head. The body was visualized using the 700 nm filter and appears red in images (Figure 3b–e). IRdye 800 can be seen within the nasal cavity as green or yellow. Yellow results from the overlap of the red 700 nm filter with the green 800 nm filter. At 0 minutes immediately after the first intranasal drop, IRdye 800 was visualized well in contrast to the transparent rat tissue (Figure 3b). At 5 minutes the IRdye 800 extends into the more caudal nasal cavity (Figure 3b). Within 10 minutes dye appears at the beginning of the olfactory bulb (Figure 3c). At 15 minutes, IRdye 800 is imaged in the rostral portion of the frontal lobe (Figure 3d). Not all of the dye in the brain imaged in figure 2 is seen in figure 3 because the Odyssey infrared imaging system cannot detect the deep ventral structures of the brain.

Trigeminal nerve and nasal cavity had high concentrations of IRdye 800 at the entry of the choana, the middle nasal concha and the maxillary sinus—Dye was visible in three locations of a mid-sagittal section of the head: the middle nasal concha, the maxillary sinus, and choana (Figure 4). High concentrations of IRdye 800 (>100 μM) were also seen at the same locations where the trigeminal nerve passes next to the middle nasal concha, maxillary sinus, and choana (Figure 4). The nerve under the middle nasal concha (>100 μM) innervates the maxillary incisors (~100 μM) and also passes through the maxillary sinus (>100 μM). Most of the nerves passing through the maxillary sinus (>100μM) innervate the whisker pad (~100 μM). The maxillary sinus (>100 μM) then connects with the nerves that pass near the choana (>100 μM) which connect to the maxillary molar nerves (~100 μM). The trigeminal nerve then passes through the cerebrospinal fluid eventually to synapse at the brainstem (~10 μM). All these values are on the same order of magnitude as the lidocaine data collected using ELISA.

Intranasal administration delivered high concentrations of IRdye 800 to the brain, particularly cerebrospinal-fluid-contacting ventral brain structures—Coronal brain sections had an IRdye 800 concentration range from 100 nM to >10 μM (Figure 2 inset), as determined by comparison to a scanned standard curve of known dye concentrations

(data not shown). Generally, ventral brain structures, near cerebrospinal fluid (CSF) were higher in IRdye 800 concentration compared to more dorsal non-CSF contacting structures. IRdye 800 distributed to the entire olfactory bulb, ventral and midline portions of the anterior olfactory nucleus, hypothalamus, medial and ventral portions of the cortex, ventral portion of the pons, and entry of trigeminal nerve roots. High concentrations of IRdye 800 concentrated in the trigeminal nuclei located on the lateral sides of the caudal brainstem and rostral cervical spinal cord.

Structures in the rest of the body received low concentrations of IRdye 800 compared to the brain and trigeminal nerve following intranasal administration —Blood contained an IRdye 800 concentration of 10 nM-100 nM. Remaining body structures, including the gastrointestinal tract, pancreas, liver, gallbladder, spleen, heart, spinal cord, kidneys, urine, epididymis and testis, had dye concentrations less than 10 nM (data not shown).

Discussion

These experiments demonstrate that intranasal delivery can target therapeutics like lidocaine to orofacial structures even more than to brain structures. This likely occurs because the trigeminal nerve acts as a conduit to transport drug from the nasal cavity to the orofacial structures. Similar to other intranasally administered molecules, low molecular weight drugs like intranasal lidocaine (234 Da) and IRdye 800 (962 Da) target the olfactory bulb, ventrally located brain structures, and the brainstem surrounding the trigeminal nerve root relative to the blood and other organs. Furthermore, this study identified three novel results. 1) Following intranasal administration, the therapeutic agent enters the trigeminal nerve and trigeminal neural pathway at three points from the nasal cavity: choana, middle nasal concha, and maxillary sinus. 2) The trigeminal neural pathway acts as a conduit to transport drug not only to the brain but also in the opposite direction to other connected structures such as the teeth and temporomandibular joint. 3) Previous experiments demonstrated intranasal administration delivers drug to the brain within 10 minutes, but this is the first experiment to *image* this phenomenon, demonstrating this transport is a rapid process. These results may aid clinicians in targeting therapeutics to the trigeminal neural pathway by administering intranasally.

Intranasal administration to an anesthetized rat concentrates drug at three major locations in the nasal cavity, which subsequently results in rapid transport across the nasal epithelium into the trigeminal neural pathway. Our study found that a small molecule concentrates (>100 μM of IRdye at 30 minutes) at certain permeable anatomical locations within the nasal cavity following intranasal delivery, particularly the entry of the choana, the middle nasal concha and the maxillary sinus.[40] Furthermore, the high concentrations within the underlying trigeminal nerve were at these exact three locations, suggesting the three high concentration regions in the nasal cavity almost exclusively penetrate drug to the trigeminal nerve. This seems plausible since a small molecule (similar in size and properties to lidocaine i.e. dopamine) has been shown to rapidly flux across the respiratory and olfactory pseudoepithelium at 2–5 μg/cm^2/min.[21, 41] Once drug enters the trigeminal neural pathway, it appears to travel to the trigeminal nerve's connected structures.

These results suggest that the trigeminal nerve is a bidirectional conduit utilized by intranasal delivery to transport therapeutic agents to connected structures: the brain and orofacial structures. Previous studies have demonstrated that drug is transported via the trigeminal nerve in a rostral-to-caudal direction to the brain,[7, 9, 10] but this is the first study to demonstrate trigeminal drug distribution in the caudal-to-rostral direction to the maxillary teeth. Based on IRdye 800 distribution data, the maxillary teeth, infraorbital nerve, temporomandibular joint, and masseter muscle receive therapeutic via the trigeminal nerve from the choana, middle nasal concha, and maxillary sinus (see Figure 4). The maxillary incisor, a more rostral structure,

showed dwindling IRdye 800 concentration emanating from the middle nasal concha and maxillary sinus, suggesting the therapeutic in the more rostral maxillary incisor originated from the more caudal middle nasal concha and maxillary sinus. The source of IRdye 800 to the maxillary molars was the choana, although there was contribution from the trigeminal nerve originating from the maxillary sinus and middle nasal concha. The infraorbital nerve had IRdye 800 concentration emanating mostly from the maxillary sinus due to the infraorbital nerve's large surface area exposed to the maxillary sinus. The IRdye 800 also appeared to transport in a rostral-to-caudal direction to the brainstem followed by a caudal-to-rostral direction to reach the temporomandibular joint and masseter muscle. All these conclusions were also supported based on the dramatically higher lidocaine tissue concentrations following intranasal delivery as compared to intravenous delivery. Thus, the trigeminal nerve, a large bundle of nerves, can be used to rapidly and non-invasively transport therapeutics to all trigeminally connected structures.

In conclusion, following intranasal administration, drug not only travels from the nasal cavity to the brain via the trigeminal neural pathway but also in the opposite direction to orofacial structures. Targeting the trigeminal neural pathway is an effective method of targeting its connected orofacial and brain structures. Intranasal delivery to the trigeminal nerve and connected orofacial structures may provide a more effective and targeted method for treating postoperative dental pain/anxiety, trigeminal neuralgia, migraine, dementia, and for vaccinating against disease.

Acknowledgments

Financial support was provided by HealthPartners Research Foundation and MinnCResT Fellowship (NIH – NIDCR T32 DE007288-13). The authors thank the various staff from the Alzheimer's Research Center at Regions Hospital: Kate Faltesek and Jodi Henthorn for assistance with animal care; Dr. Shyeilla Dhuria for training on surgical procedures; Aleta Svitak, Rachel Matthews, Thuhien Nguyen, and Dianne Marti, for assistance with tissue fixation and dissection; and Yevgenia Friedman for preparation of fixative solutions. We thank Jared Fine, PhD for critical review of the manuscript and aid in IRdye 800 experiments. We thank Marie Johnson and Cheryl Johnson for tube weighing and moral support, and Charley Little for graphic design & art direction for figure 4.

Abbreviations

PBS	phosphate buffered saline
CNS	central nervous system
IN	intranasal
TMD	temporomandibular disorder
DTI	drug-targeting index
CSF	cerebrospinal fluid

References

1. Capsoni S, Giannotta S, Cattaneo A. Nerve growth factor and galantamine ameliorate early signs of neurodegeneration in anti-nerve growth factor mice. Proc Natl Acad Sci USA 2002;99(19):12432. [PubMed: 12205295]
2. De Rosa R, Garcia AA, Braschi C, Capsoni S, Maffei L, Berardi N, Cattaneo A. Intranasal administration of nerve growth factor (NGF) rescues recognition memory deficits in AD11 anti-NGF transgenic mice. Proc Natl Acad Sci USA 2005;102(10):3811. [PubMed: 15728733]
3. Hanson LR, Frey WH. 2nd, Intranasal delivery bypasses the blood-brain barrier to target therapeutic agents to the central nervous system and treat neurodegenerative disease. BMC Neurosci 2008;9(Suppl 3):S5. [PubMed: 19091002]

4. Hanson L, Roeytenberg A, Martinez PM, Coppes VG, Sweet DC, Rao RJ, Marti DL, Hoekman JD, Matthews RB, Frey WH, Panter SS. Intranasal deferoxamine provides increased brain exposure and significant protection in rat ischemic stroke. J Pharmacol Exp Ther. 2009
5. Hashizume R, Ozawa T, Gryaznov SM, Bollen AW, Lamborn KR, Frey WH 2nd, Deen DF. New therapeutic approach for brain tumors: Intranasal delivery of telomerase inhibitor GRN163. Neuro Oncol 2008;10(2):112. [PubMed: 18287341]
6. Liu XF, Fawcett JR, Hanson LR, Frey WH. 2nd, The window of opportunity for treatment of focal cerebral ischemic damage with noninvasive intranasal insulin-like growth factor-I in rats. J Stroke Cerebrovasc Dis 2004;13(1):16. [PubMed: 17903945]
7. Thorne RG, Pronk GJ, Padmanabhan V, Frey WH. 2nd, Delivery of insulin-like growth factor-I to the rat brain and spinal cord along olfactory and trigeminal pathways following intranasal administration. Neuroscience 2004;127(2):481. [PubMed: 15262337]
8. Jerusalmi A, Morris-Downes MM, Sheahan BJ, Atkins GJ. Effect of intranasal administration of Semliki Forest virus recombinant particles expressing reporter and cytokine genes on the progression of experimental autoimmune encephalomyelitis. Mol Ther 2003;8(6):886–94. [PubMed: 14664790]
9. Ross TM, Martinez PM, Renner JC, Thorne RG, Hanson LR, Frey WH 2nd. Intranasal administration of interferon beta bypasses the blood-brain barrier to target the central nervous system and cervical lymph nodes: a non-invasive treatment strategy for multiple sclerosis. J Neuroimmunol 2004;151(1–2):66. [PubMed: 15145605]
10. Thorne RG, Hanson LR, Ross TM, Tung D, Frey WH 2nd. Delivery of interferon-beta to the monkey nervous system following intranasal administration. Neuroscience 2008;152(3):785. [PubMed: 18304744]
11. Reger MA, Watson GS, Frey WH 2nd, Baker LD, Cholerton B, Keeling ML, Belongia DA, Fishel MA, Plymate SR, Schellenberg GD, Cherrier MM, Craft S. Effects of intranasal insulin on cognition in memory-impaired older adults: modulation by APOE genotype. Neurobiol Aging 2006;27(3):451. [PubMed: 15964100]
12. Deadwyler SA, Porrino L, Siegel JM, Hampson RE. Systemic and nasal delivery of orexin-A (Hypocretin-1) reduces the effects of sleep deprivation on cognitive performance in nonhuman primates. J Neurosci 2007;27(52):14239–47. [PubMed: 18160631]
13. Born J, Lange T, Kern W, McGregor GP, Bickel U, Fehm HL. Sniffing neuropeptides: a transnasal approach to the human brain. Nat Neurosci 2002;5(6):514. [PubMed: 11992114]
14. Benedict C, Hallschmid M, Hatke A, Schultes B, Fehm HL, Born J, Kern W. Intranasal insulin improves memory in humans. Psychoneuroendocrinology 2004;29(10):1326. [PubMed: 15288712]
15. Benedict C, Hallschmid M, Schmitz K, Schultes B, Ratter F, Fehm HL, Born J, Kern W. Intranasal insulin improves memory in humans: superiority of insulin aspart. Neuropsychopharmacology 2007;32(1):239. [PubMed: 16936707]
16. Benedict C, Kern W, Schultes B, Born J, Hallschmid M. Differential sensitivity of men and women to anorexigenic and memory-improving effects of intranasal insulin. J Clin Endocrinol Metab 2008;93(4):1339. [PubMed: 18230654]
17. Hallschmid M, Benedict C, Schultes B, Born J, Kern W. Obese men respond to cognitive but not to catabolic brain insulin signaling. Int J Obes(Lond) 2008;32(2):275. [PubMed: 17848936]
18. Reger MA, Watson GS, Green PS, Baker LD, Cholerton B, Fishel MA, Plymate SR, Cherrier MM, Schellenberg GD, Frey WH 2nd, Craft S. Intranasal insulin administration dose-dependently modulates verbal memory and plasma amyloid-beta in memory-impaired older adults. J Alzheimers Dis 2008;13(3):323. [PubMed: 18430999]
19. Reger MA, Watson GS, Green PS, Wilkinson CW, Baker LD, Cholerton B, Fishel MA, Plymate SR, Breitner JC, DeGroodt W, Mehta P, Craft S. Intranasal insulin improves cognition and modulates beta-amyloid in early AD. Neurology 2008;70(6):440. [PubMed: 17942819]
20. Reger MA, Craft S. Intranasal insulin administration: a method for dissociating central and peripheral effects of insulin. Drugs Today (Barc) 2006;42(11):729–39. [PubMed: 17171192]
21. Chemuturi NV, Donovan MD. Role of organic cation transporters in dopamine uptake across olfactory and nasal respiratory tissues. Mol Pharm 2007;4(6):936–42. [PubMed: 17892261]

22. Kyrkanides S, Yang M, Tallents RH, Miller JN, Brouxhon SM, Olschowka JA. The trigeminal retrograde transfer pathway in the treatment of neurodegeneration. J Neuroimmunol 2009;209(1–2): 139–42. [PubMed: 19278737]
23. Tfelt-Hansen P. Early Responses in Randomized Clinical Trials of Triptans in Acute Migraine Treatment. Are They Clinically Relevant? A Comment. Headache. 2008
24. Rapoport A, Winner P. Nasal delivery of antimigraine drugs: clinical rationale and evidence base. Headache 2006;46(Suppl 4):S192–201. [PubMed: 17078851]
25. Gawel M, Aschoff J, May A, Charlesworth BR. Zolmitriptan 5 mg nasal spray: efficacy and onset of action in the acute treatment of migraine--results from phase 1 of the REALIZE Study. Headache 2005;45(1):7–16. [PubMed: 15663607]
26. Rapoport A. The sumatriptan nasal spray: a review of clinical trials. Cephalalgia 2001;21(Suppl 1): 13–5. [PubMed: 11678814]
27. Dowson AJ, Charlesworth BR, Green J, Farkkila M, Diener HC, Hansen SB, Gawel M. Zolmitriptan nasal spray exhibits good long-term safety and tolerability in migraine: results of the INDEX trial. Headache 2005;45(1):17–24. [PubMed: 15663608]
28. Dowson AJ, Charlesworth BR, Purdy A, Becker WJ, Boes-Hansen S, Farkkila M. Tolerability and consistency of effect of zolmitriptan nasal spray in a long-term migraine treatment trial. CNS Drugs 2003;17(11):839–51. [PubMed: 12921494]
29. Charlesworth BR, Dowson AJ, Purdy A, Becker WJ, Boes-Hansen S, Farkkila M. Speed of onset and efficacy of zolmitriptan nasal spray in the acute treatment of migraine: a randomised, double-blind, placebo-controlled, dose-ranging study versus zolmitriptan tablet. CNS Drugs 2003;17(9):653–67. [PubMed: 12828501]
30. Rapoport AM, Mathew NT, Silberstein SD, Dodick D, Tepper SJ, Sheftell FD, Bigal ME. Zolmitriptan nasal spray in the acute treatment of cluster headache: a double-blind study. Neurology 2007;69(9): 821–6. [PubMed: 17724283]
31. Rapoport AM, Bigal ME, Tepper SJ, Sheftell FD. Intranasal medications for the treatment of migraine and cluster headache. CNS Drugs 2004;18(10):671–85. [PubMed: 15270595]
32. Rothner AD, Winner P, Nett R, Asgharnejad M, Laurenza A, Austin R, Peykamian M. One-year tolerability and efficacy of sumatriptan nasal spray in adolescents with migraine: results of a multicenter, open-label study. Clin Ther 2000;22(12):1533–46. [PubMed: 11192144]
33. Winner P, Rothner AD, Saper J, Nett R, Asgharnejad M, Laurenza A, Austin R, Peykamian M. A randomized, double-blind, placebo-controlled study of sumatriptan nasal spray in the treatment of acute migraine in adolescents. Pediatrics 2000;106(5):989–97. [PubMed: 11061765]
34. Gilchrist F, Cairns AM, Leitch JA. The use of intranasal midazolam in the treatment of paediatric dental patients. Anaesthesia 2007;62(12):1262–5. [PubMed: 17991264]
35. Christensen K, Cohen A, Mermelstein F, Hamilton D, McNicol E, Babul N, Carr D. The analgesic efficacy and safety of a novel intranasal morphine formulation (morphine plus chitosan), immediate release oral morphine, intravenous morphine, and placebo in a postsurgical dental pain model. Anesthesia & Analgesia 2008;107(6):2018. [PubMed: 19020153]
36. Maizels M. Intranasal lidocaine to prevent headache following migraine aura. Headache 1999;39(6): 439–42. [PubMed: 11279923]
37. Maizels M, Scott B, Cohen W, Chen W. Intranasal lidocaine for treatment of migraine: a randomized, double-blind, controlled trial. JAMA 1996;276(4):319–21. [PubMed: 8656545]
38. Kanai A, Suzuki A, Kobayashi M, Hoka S. Intranasal lidocaine 8% spray for second-division trigeminal neuralgia. British Journal of Anaesthesia 2006;97(4):559. [PubMed: 16882684]
39. Maizels M, Geiger AM. Intranasal lidocaine for migraine: a randomized trial and open-label follow-up. Headache 1999;39(8):543–51. [PubMed: 11279969]
40. Edranov SS, Kovalyeva IV, Kryukov KI, Konovko AA. Anatomic and histological study of maxillary sinus in albino rat. Bull Exp Biol Med 2004;138(6):603–6. [PubMed: 16134824]
41. Dahlin M, Jansson B, Bjork E. Levels of dopamine in blood and brain following nasal administration to rats. Eur J Pharm Sci 2001;14(1):75–80. [PubMed: 11457653]
42. Dhanda DS, FWI, Leopold D, Kompella UB. Approaches for drug deposition in the human olfactory epithelium. Drug Del Tech 2005;5:64–72.

43. Capsoni S, Giannotta S, Cattaneo A. Beta-amyloid plaques in a model for sporadic Alzheimer's disease based on transgenic anti-nerve growth factor antibodies. Mol Cell Neurosci 2002;21(1):15. [PubMed: 12359148]
44. Vlckova I, Navratil P, Kana R, Pavlicek P, Chrbolka P, Djupesland PG. Effective treatment of mild-to-moderate nasal polyposis with fluticasone delivered by a novel device. Rhinology 2009;47(4): 419–426. [PubMed: 19936370]
45. Djupesland PG, Skretting A, Winderen M, Holand T. Breath actuated device improves delivery to target sites beyond the nasal valve. Laryngoscope 2006;116(3):466–72. [PubMed: 16540911]
46. Bakke H, Samdal HH, Holst J, Oftung F, Haugen IL, Kristoffersen AC, Haugan A, Janakova L, Korsvold GE, Krogh G, Andersen EA, Djupesland P, Holand T, Rappuoli R, Haneberg B. Oral spray immunization may be an alternative to intranasal vaccine delivery to induce systemic antibodies but not nasal mucosal or cellular immunity. Scand J Immunol 2006;63(3):223–31. [PubMed: 16499576]
47. Djupesland PG, Skretting A, Winderen M, Holand T. Bi-directional nasal delivery of aerosols can prevent lung deposition. J Aerosol Med 2004;17(3):249–59. [PubMed: 15625817]
48. Giroux M, Hwang P, Prasad A. Controlled Particle Dispersionô: applying vortical flow to optimize nasal drug deposition. Drug Deliv Technol 2005;5:44–49.
49. Caffey, J. Pediatric X-Ray Diagnosis. Year Book Medical Publishers; Chicago: 1967.
50. Rice, DH. Embryology. In: Donald, PJ.; Gluckman, JL.; Rice, DH., editors. The Sinuses. Raven Press; New York: 1995. p. 21
51. Porter, G.; Quinn, FB. Paranasal Sinus Anatomy and Function. In: Quinn, FB.; Ryan, MW., editors. Grand Rounds Presentation, UTMB, Department of Otolaryngology. Galveston, Texas: 2002.
52. Burstein A, Modica R, Hatton M, Forrest A, Gengo F. Pharmacokinetics and pharmacodynamics of midazolam after intranasal administration. The Journal of Clinical Pharmacology 1997;37(8):711–718.
53. Lee-Kim S, Fadavi S, Punwani I, Koerber A. Nasal Versus Oral Midazolam Sedation Pediatric Dental Patients. JOURNAL OF DENTISTRY FOR CHILDREN-NEW SERIES 2004;71:126–130.
54. Sindrup SH, Jensen TS. Pharmacotherapy of trigeminal neuralgia. Clin J Pain 2002;18(1):22. [PubMed: 11803299]
55. Finnerup NB, Otto M, McQuay HJ, Jensen TS, Sindrup SH. Algorithm for neuropathic pain treatment: an evidence based proposal. Pain 2005;118(3):289–305. [PubMed: 16213659]
56. Lewis MA, Sankar V, De Laat A, Benoliel R. Management of neuropathic orofacial pain. Oral Surg Oral Med Oral Pathol Oral Radiol Endod 2007;103(Suppl):S32e1–24. [PubMed: 17379152]
57. Barakat NS, Omar SA, Ahmed AA. Carbamazepine uptake into rat brain following intra-olfactory transport. J Pharm Pharmacol 2006;58(1):63–72. [PubMed: 16393465]
58. Gavini E, Hegge AB, Rassu G, Sanna V, Testa C, Pirisino G, Karlsen J, Giunchedi P. Nasal administration of carbamazepine using chitosan microspheres: in vitro/in vivo studies. Int J Pharm 2006;307(1):9–15. [PubMed: 16257156]
59. Kudrow L, Kudrow DB, Sandweiss JH. Rapid and sustained relief of migraine attacks with intranasal lidocaine: preliminary findings. Headache 1995;35(2):79–82. [PubMed: 7737865]
60. Whalen RL, Dempsey DJ, Thompson LM, Bucknell K, Kunitomo R, Okazaki Y, Harasaki H. Microencapsulated vaccines to provide prolonged immunity with a single administration. ASAIO J 1996;42(5):M649–54. [PubMed: 8944961]

Illustrations embedded in the manuscript:

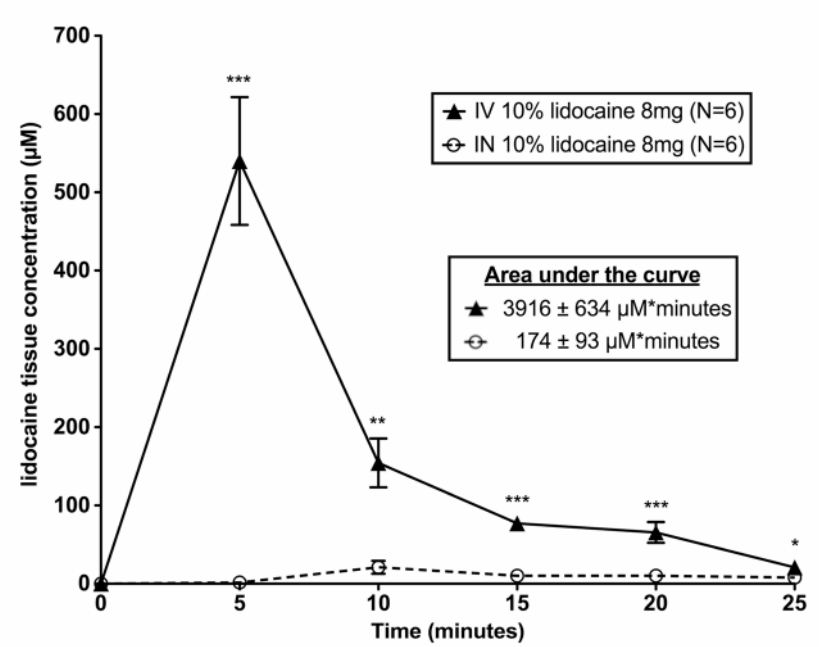

Figure 1. Intranasal administration of lidocaine leads to less drug delivery to the blood as compared to intravenous administration

Following intranasal or intravenous delivery of 8 mg of 10% lidocaine, lidocaine concentrations in the blood were measured every 5 minutes. For intranasal delivery the area under the curve of lidocaine concentration in the blood over the 25 minute period was 174±93 μM*seconds, and intravenous delivery had an area under the curve of 3916±634 μM*seconds. Intranasal delivery had significantly less lidocaine from 0–25 minutes compared to IV delivery ($p<0.001$). The points and error bars represent the mean ± SEM (N=6). P values are represented as follows: <0.05 (*), <0.01 (**), and <0.001(***).

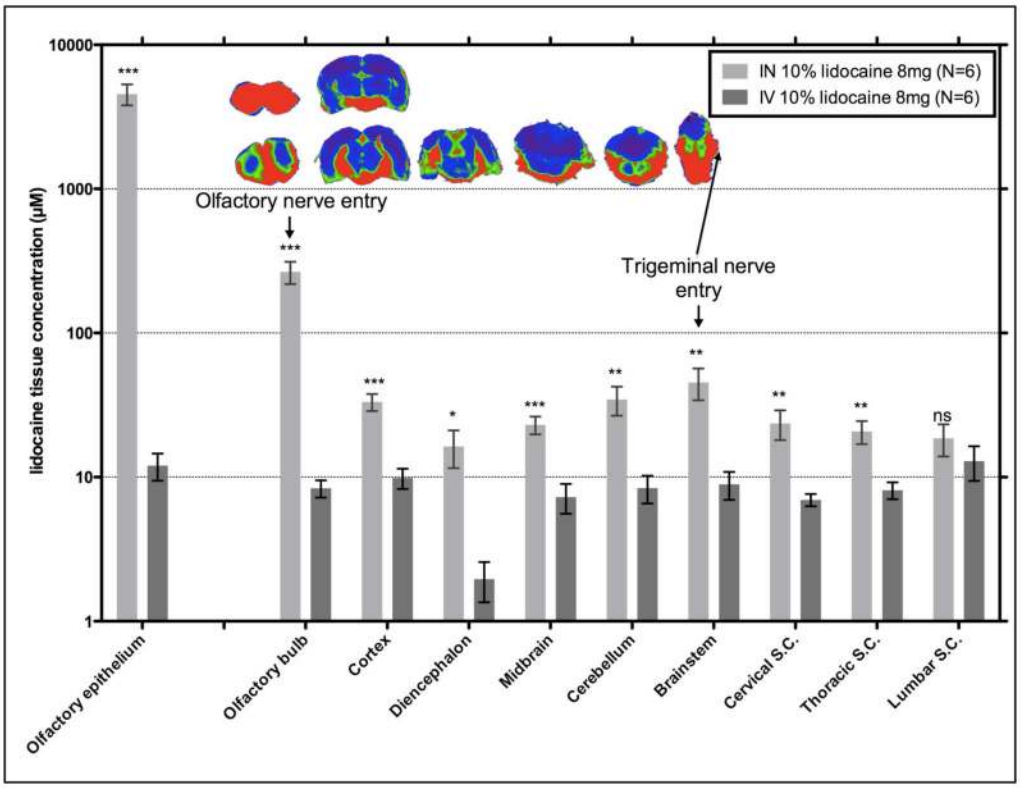

Figure 2. Brain structures had higher lidocaine tissue concentrations following intranasal delivery as compared to intravenous delivery, and accumulated around the olfactory nerves, trigeminal nerves, and cerebrospinal fluid

The bars are grouped by tissue comparing delivery method (intranasal or intravenous) of 8 mg of a 10% lidocaine solution with the error bars as SEM (N=6). P values are represented as follows: <0.05 (*), <0.01 (**), and <0.001 (***). The coronal brain sections in the inset illustrate the distribution within these brain structures where high concentrations are visualized in regions of the brain in contact with CSF, olfactory nerve, and trigeminal nerve.

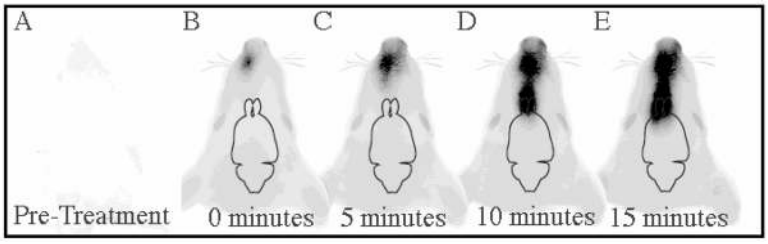

Figure 3. Distribution time course of intranasal delivery to the brain

At 800 nm an anesthetized rat is relatively transparent using an Odyssey infrared imaging system (A). At 0 minutes after the first 1mM drop was delivered it was clearly seen at an 800 nm wavelength (B). At 5 minutes the IRdye can be clearly seen in the nasal cavity (C). At 10 minutes IRdye 800 enters the olfactory bulb (D). At 15 minutes IRdye 800 enters the cortex (E). There were no significant changes in IRdye 800 distribution between 15, 20 and 25 minutes. Every 2 minutes an 8μL drop was administered.

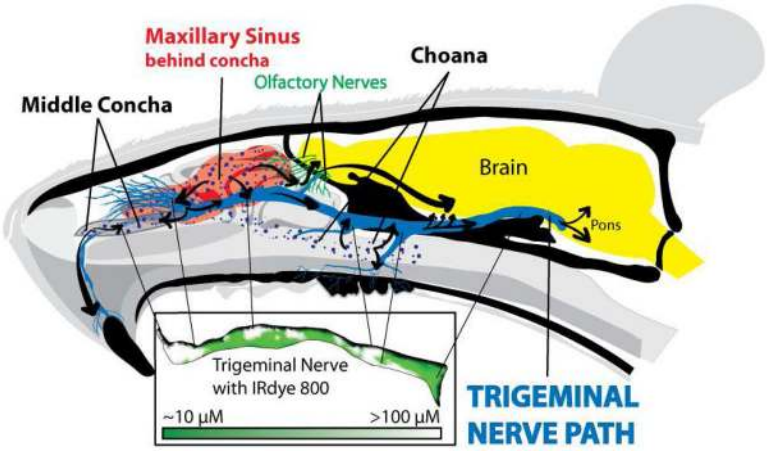

Figure 4. Intranasal administration delivers IRdye 800 to the trigeminal nerve and maxillary teeth via the middle concha, maxillary sinus, and choana

Intranasal delivery deposits IRdye 800 in three locations: middle concha, maxillary sinus and choana. After intranasal administration, IRdye 800 (purple dots) passes under the middle nasal concha and into the maxillary sinus (in red). Upon contact with the middle nasal concha and maxillary sinus, the underlying incisal nerve and multi-branched infraorbital nerve absorb >100 µM IRdye. After entering these structures the dye is transported in both directions along the trigeminal nerve. The remaining IRdye 800 is deposited in the choana where it is distributed to the maxillary molar and septal nerve branches. As IRdye is transported to the brainstem, IRdye 800 concentration plummets as it is deposited into the base of the skull and CSF. The cribriform plate also had a high concentration of IRdye 800. The trigeminal nerve (see inset) has high IRdye 800 concentrations in four locations: 1) the maxillary incisal nerve as it passes through the middle concha, 2) the infraorbital nerve as it passes through the maxillary sinus, 3) the septal branch and 4) maxillary molar branch as they passes through the choana. The maxillary teeth and trigeminal nerve receive IRdye based on its proximity from these trigeminally connected structures.

Mol Pharm. Author manuscript; available in PMC 2011 June 7.

Table 1

Lidocaine tissue concentrations following intranasal or intravenous administration

The table shows the mean and SEM (N=6) of tissue concentrations following intranasal and intravenous administration. The p values for each tissue is an unpaired t-test comparison between intranasal and IV delivery (<0.05 (*), <0.01 (**), & <0.001 (***).

	Lidocaine tissue concentration (μM)					Lidocaine targeting: ratio of tissue concentration (μM)/blood concentration at 25 minutes (μM)				Drug Targeting Index
	IN 10% lidocaine 8mg (N=6)		IV 10% lidocaine 8mg (N=6)			IN 10% lidocaine 8mg (N=6)		IV 10% lidocaine 8mg (N=6)		Ratio IN/IV
Tissue	Mean	± SEM (μM)	Mean	± SEM (μM)	Significance	Mean	± SEM	Mean	± SEM	Mean
Blood										
Blood 5min	1.6	± 0.7	540	± 82	***					
Blood 10min	21	± 8.3	154	± 31	**					
Blood 15min	10	± 4.6	77	± 8.0	***					
Blood 20min	10	± 3.2	65	± 13	***					
Blood 25min	7.9	± 1.8	21	± 3.3	*					
Total area under the curve (0–25 minutes) μM*minutes	173	± 93	3,916	± 634	***					
Peripheral Tissues										
Deep Cervical Lymph Nodes	30	± 5.9	13	± 1.6	*	3.8	± 3.2	0.6	± 0.5	6.2
Nasal epithelium	4,549	± 756	12	± 2.6	***	577	± 409	0.6	± 0.8	1003
Urine	48	± 13	1,142	± 318	**	6.1	± 6.9	55	± 97	0.1
Kidney	80	± 7.6	88	± 16	ns	10	± 4.1	4.2	± 5.0	2.4
Liver	44	± 5.0	87	± 11	**	5.6	± 2.7	4.1	± 3.2	1.3
Brain and Spinal Cord Tissue										
Olfactory Bulb	266	± 47	8.4	± 1.1	***	34	± 25	0.4	± 0.3	84
Cortex	33	± 4.5	9.9	± 1.6	***	4.2	± 2.4	0.5	± 0.5	8.9
Diencephalon	16	± 4.8	2.0	± 0.6	**	2.1	± 2.6	0.1	± 0.2	22
Midbrain	23	± 3.2	7.3	± 1.7	***	2.9	± 1.8	0.3	± 0.5	8.4
Cerebellum	35	± 7.9	8.4	± 1.8	**	4.4	± 4.3	0.4	± 0.6	11
Brainstem and upper S.C.	45	± 11	8.9	± 2.0	**	5.8	± 6.1	0.4	± 0.6	14
Lower cervical S.C.	24	± 5.5	7.0	± 0.7	**	3.0	± 3.0	0.3	± 0.2	9.0
Thoracic S.C.	21	± 3.8	8.1	± 1.1	**	2.6	± 2.0	0.4	± 0.3	6.8
Lumbar S.C.	19	± 4.7	13	± 3.5	ns	2.4	± 2.5	0.6	± 1.1	3.8

	Lidocaine tissue concentration (μM)					Lidocaine targeting: ratio of tissue concentration (μM)/blood concentration at 25 minutes (μM)				Drug Targeting Index
	IN 10% lidocaine 8mg (N=6)		IV 10% lidocaine 8mg (N=6)			IN 10% lidocaine 8mg (N=6)		IV 10% lidocaine 8mg (N=6)		Ratio IN/IV
Tissue	**Mean**	**± SEM (μM)**	**Mean**	**± SEM (μM)**	**Significance**	**Mean**	**± SEM**	**Mean**	**± SEM**	**Mean**
Trigeminal ganglion[a]	147	± 44	13	± 1.5	**	19	± 24	0.6	± 0.5	29
Oral structures with trigeminal innervations										
Maxillary Sinus	3,508	± 685	11	± 2.4	***	445	± 371	0.5	± 0.7	856
Maxillary Incisor - SA nerve (V2)	803	± 253	3.0	± 0.5	**	102	± 137	0.1	± 0.2	701
Maxillary Molar - SA nerve (V2)	476	± 116	3.1	± 0.4	***	60	± 63	0.1	± 0.1	413
Mandibular Incisor - IA nerve (V3)	148	± 31	2.7	± 0.6	***	19	± 17	0.1	± 0.2	145
Mandibular Molar - IA nerve (V3)	199	± 43	1.9	± 0.8	***	25	± 24	0.1	± 0.2	270
Tongue (V3)	651	± 35	8.1	± 1.6	***	83	± 19	0.4	± 0.5	213
Facial structures with trigeminal innervations										
Temporomandibular joint (V3)	72	± 27	7.1	± 1.0	***	9.1	± 15	0.3	± 0.3	27
Masseter muscle (V3)	15	± 2.7	4.8	± 0.8	*	1.9	± 1.4	0.2	± 0.2	8.2
Lacrimal gland (VII)	58	± 14	43	± 4.4	ns	7.4	± 7.6	2.0	± 1.4	3.6
Skin and aponeurosis on Head (V1)	3.6	± 1.1	3.6	± 0.5	ns	0.5	± 0.6	0.2	± 0.2	2.7
Eye (V1 and CN II)	8.3	± 1.5	6.5	± 0.7	ns	1.1	± 0.8	0.3	± 0.2	3.4

Significance = <0.05 (*), <0.01 (**), <0.001 (***)

[a]The trigeminal nerve was dissected at the base of the skull. See Figure 4 for concentration distribution in the trigeminal nerve.

Mol Pharm. Author manuscript; available in PMC 2011 June 7.